SCIENTIFIC REPORTS

OPEN

SUBJECT AREAS:
GEOMORPHOLOGY
PALAEOCLIMATE
ENVIRONMENTAL SCIENCES
SEDIMENTOLOGY

Received
13 August 2014

Accepted
20 November 2014

Published
8 December 2014

Correspondence and requests for materials should be addressed to C.M.B. (cbrandon@geo.umass.edu)

How Unique was Hurricane Sandy? Sedimentary Reconstructions of Extreme Flooding from New York Harbor

Christine M. Brandon[1], Jonathan D. Woodruff[1], Jeffrey P. Donnelly[2] & Richard M. Sullivan[2]

[1]Department of Geosciences, 611 N. Pleasant St., 233 Morrill Science Center, University of Massachusetts Amherst, Amherst, MA, 01003, USA, [2]Department of Geology and Geophysics, Mail Stop #22, Woods Hole Oceanographic Institution, Woods Hole, MA, 02543, USA.

The magnitude of flooding in New York City by Hurricane Sandy is commonly believed to be extremely rare, with estimated return periods near or greater than 1000 years. However, the brevity of tide gauge records result in significant uncertainties when estimating the uniqueness of such an event. Here we compare resultant deposition by Hurricane Sandy to earlier storm-induced flood layers in order to extend records of flooding to the city beyond the instrumental dataset. Inversely modeled storm conditions from grain size trends show that a more compact yet more intense hurricane in 1821 CE probably resulted in a similar storm tide and a significantly larger storm surge. Our results indicate the occurrence of additional flood events like Hurricane Sandy in recent centuries, and highlight the inadequacies of the instrumental record in estimating current flood risk by such extreme events.

On October 29, 2012 Hurricane Sandy inundated New York City, NY, raising water levels to 3.4 m above 2012 mean sea level (MSL) at the Battery (located at the south end of lower Manhattan). The return period of this storm tide is estimated to be 1570 years based on generalized extreme value return curves from existing tide gauge data[1], and simulated hurricane climatology ranks this storm as a 1-in-900 year event[2]. However, tide gauge data alone is generally too short to either obtain accurate extreme value statistics or evaluate the skill of extreme flood probabilities derived solely from numerical simulations[3]. Thus there is a real need for longer flood reconstructions, particularly for critically important coastlines like New York City. Historical documentation of storm activity for the city (i.e. newspapers, nautical logs, etc.) can extend storm records back to the mid-1600s for the U.S. east coast[4–7]. While these records provide valuable information on the occurrence of storms, detailed quantitative information on specific storm characteristics prior to 1844[8] is limited, particularly with respect to flood magnitudes.

Storm surge and storm tide are two separate metrics that describe the storm-induced rise in water levels. Storm surge is the anomalous rise in water level above the predicted astronomical tide (excluding the impacts of waves), and storm tide is the total rise in water level due to the combination of storm surge and astronomical tides. Hurricane Sandy's peak hourly averaged water levels occurred at high tide at the Battery with a storm tide of 3.4 m above 2012 MSL and a storm surge of 2.8 m. Peak monthly water levels verified by the National Oceanic and Atmospheric Administration (NOAA) extend back to 1927 CE, and with the merging of an additional nearby tide gauge, provide a reconstruction of peak annual flood heights at the Battery back to 1893 CE[9]. Hurricane Sandy's storm tide exceeded past maxima in these records by over 1 meter (Hurricane Donna's 1960 CE storm tide held the previous record at 2.3 m).

Sandy's storm surge was also record breaking but to a lesser degree, exceeding the previous maxima in the vetted NOAA data set by roughly 40 cm (the Great Appalachian Storm of 1950 was the previous storm surge of record at 2.4 m). A more recent analysis of archived tide gauge data from the New York City area extends storm tide and storm surge records for the Battery back to 1844 and 1860 CE, respectively[8], with Hurricane Sandy remaining the event of record in both.

While Hurricane Sandy was record breaking compared to published tide gauge records, earlier historical accounts suggest that a major hurricane in 1821 CE may have had a similar storm tide and a substantially larger storm surge[5,7]. During this 1821 hurricane the *New Bedford Mercury* newspaper reported a rise in water of 13 feet 4 inches or 4.06 m above low water in the East River[4,6]. The 1821 hurricane struck New York City at low tide with roughly 4.0 to 4.1 m of storm surge, compared to Sandy's 2.8 m of storm surge. Assuming this account is

referenced to near the Battery, a 4.0 m storm surge would far exceed all events recorded within the instrumental tide gauge record, including Hurricane Sandy. Other flood descriptions support the 1821 hurricane as a significant flood event, including a 10 foot (3.0 m) rise in water level at Pungoteague, VA[5], drift caught in the trees 9 feet (2.7 m) above the ground at Cape May, NJ[5], and a tide several feet above normal at New London, CT[6]. Because peak flooding for the 1821 hurricane occurred at low tide, its storm tide was smaller than its overall surge. Ref. 7 estimated a storm tide of roughly 3.2 m for the event, which is slightly less than that observed for Hurricane Sandy at 3.4 m.

Proxy records of extreme storm surge, such as overwash deposits preserved in coastal ponds and marshes, provide the opportunity for an independent assessment of early historical flood events[10–18]. Specific to the New York City region, ref. 7 developed a proxy record of hurricane flooding just to the east of the city using dated storm deposits preserved within a series of back-barrier saltmarshes in western Long Island. This reconstruction contained evidence of four significant flood events within the early historic period that were attributed to hurricane strikes in 1693, 1788, 1821 and 1893. Sedimentary reconstructions from the central coast of New Jersey contain evidence for the 1821 event and/or a hurricane in 1788, but no deposits associated with the 1893 and 1693 hurricanes[18]. The lack of evidence regarding a significant 1893 flood for New York City is also consistent with the recent analysis of archived tide gauge data[8], which, when combined with the Long Island and New Jersey storm proxies, suggest that the 1893 flood event may have been focused farther to the east along Long Island.

Discrepancies between archived tide gauge data in New York Harbor and the dated 1893 storm deposits on Long Island highlight the need for flood reconstructions obtained directly from New York Harbor itself. Furthermore, an important component to any paleostorm reconstruction is the ability to sample and analyze a modern deposit laid down by an event of known intensity. Derived sedimentary proxies of hurricane overwash from the modern Sandy layer, therefore, are extremely valuable for improved identification and analyses of older storm deposits preserved in the region. Towards this end, we present here the first sedimentary reconstruction of significant flooding in New York Harbor based on event deposits preserved within a back-barrier pond on Staten Island, and informed with recent deposition in 2012 by Hurricane Sandy.

Local Geology and Field Site. Staten Island, one of the five boroughs of New York City, is located along the west side of New York Harbor (Fig. 1a). Proper interpretations of overwash deposition on the island require some background on its glacial legacy. The Harbor Hill terminal moraine, which forms the island's southwestern coast, was deposited during the Last Glacial Maximum and marks the southernmost extent of the Laurentide ice sheet[19] (Fig. 1b). Grain sizes within the Harbor Hill moraine are poorly sorted, ranging in size from clay to boulder. Most of the fine grains within this reddish-brown till (which gets its distinctive color from an abundance of hematite) are derived from the Triassic "red beds" located directly to the north[20].

Seguine Pond is a small ~1.2 m deep coastal, back-barrier pond on the southern coast of Staten Island (Fig. 1c). The pond occupies a narrow, drowned fluvial valley that cuts through the terminal moraine. A small, 250 m long barrier beach roughly 1–2 m in height forms the southern shore of the pond and separates it from the open waters of Lower New York Bay. This 20–40 m wide barrier beach is secured in place on either end by two coastal bluffs composed of glacial till. The barrier is fairly uniform in height with the exception of a narrow (~5 m wide) topographic low at its eastern end, which serves as an occasional freshwater outlet for the pond.

A small stream network drains into the north side of the pond with a total catchment area of roughly 1 sq. km[21]. The Seguine catchment is currently composed primarily of lowland suburban terrain draining initially into conservation marshlands. These wetlands are interrupted by a series of deeper natural kettle and artificial retention ponds, which both provide internal sediment traps that likely limit stream-borne fluxes directly into Seguine Pond.

Results

Hurricane Sandy's Impact at Seguine Pond. An interpolation of surveyed high water marks collected by the United States Geological Survey after Hurricane Sandy highlight how storm surges are amplified in the New York Bight region, particularly within funnel-shaped embayments tapering to the west (Fig. 1a). Such is the case in Raritan Bay, along the west side of New York City's Lower Harbor, and bordering the southern side of Staten Island. This area experienced the highest storm tide in New York (Fig. 1a), with a range between 3.7 and 4.0 m above 2012 MSL for Staten Island's southern coast[22].

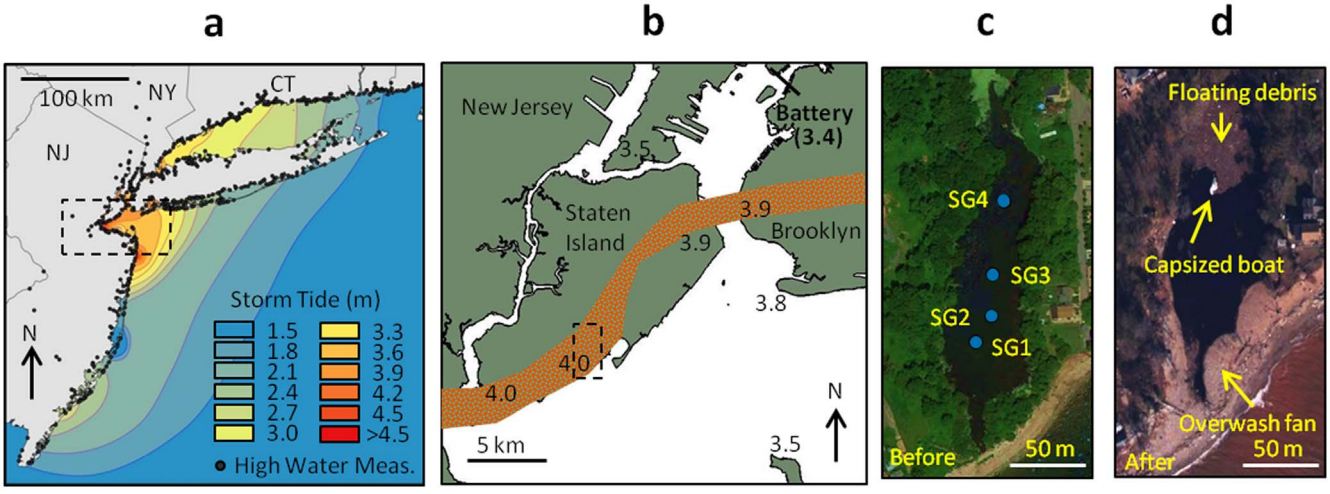

Figure 1 | The Field Site. (a) Hurricane Sandy's storm surge, based on an interpolation between USGS high water measurements (black dots) using ArcGIS 10.0. Note that the offshore contours are extensions of these onshore observations, with uncertainty increasing with distance offshore. Upper scale bar is 100 km. Box shows the area indicated in b. (b) Location of Seguine Pond on the southern coast of Staten Island. Lower scale bar is 5 km. Brown area indicates the extent of the terminal moraine. Numbers are selected USGS high water marks for Hurricane Sandy given in meters above NAVD88. Box shows the area indicated in c and d. (c) Landsat satellite image of Seguine Pond in 2010 with core locations shown. Scale bar is 50 m. (d) Seguine Pond on Nov. 4, 2012, 6 days post-Sandy. Scale bar is 50 m.

Satellite and aircraft images acquired both prior to and immediately after the event highlight the effect of the storm on coastal environments[23]. Specific to Seguine Pond, two newly deposited overwash fans are evident along the backside of the fronting barrier, with widespread marine-derived debris floating within the pond (Fig. 1d). Much of the coastline surrounding the site was stripped of its vegetation during the storm, exposing escarpments of reddish-brown till along the coastal bluffs. Fine grained sediment from these newly eroded escarpments can be seen advecting away from the coast as reddish plumes in post-Sandy images.

Chronological Constraints. Shortly following Hurricane Sandy four cores were extracted from Seguine Pond along a shore-normal transect (Fig. 1c). Deposition associated with the storm was evident within all surficial sediments. In core photographs and x-radiographs the deposit can be identified as a surficial layer of red, anomalously dense sediment (Fig. 2a, b). The reddish color of the deposit is interpreted to represent the enrichment in fine-grained hematite eroded directly from the glacial till composing the site's coastal bluffs and the deposit's higher density is due to its low organic content (and in turn higher clastic content) relative to underlying material. The Sandy deposit is also identified by anomalously low mercury (Hg) and zinc (Zn) concentrations, two industrially derived heavy metals (Fig. 2c, d). The deposit's concurrent drop in Hg and Zn are most likely due to the low levels of contaminants within the clastic beach and glacial sediments from which the deposit is primarily derived[24].

We use carbon-14 (^{14}C), cesium-137 (^{137}Cs), and the onset of Hg and Zn to temporally constrain the ages of the inundation deposits. Beginning at the sediment surface and moving down core, age constraints for the central core site (SG2, Fig. 1c) begin with the 2012 base of the Hurricane Sandy deposit at a depth of 8 cm (Fig. 2 and 3). The peak in ^{137}Cs associated with the 1963 CE peak in atmospheric nuclear testing is observed farther down at a depth of 67 cm, followed by the onset for ^{137}Cs at 75 cm associated with the onset of atmospheric nuclear testing in 1954 CE[25]. Hg and Zn concurrently begin to rise in core SG2 above a sediment depth of 114 cm, which has been identified previously as the 1850–1900 CE onset of industrialization[26,27,28]. Finally, a radiocarbon sample collected at 200 cm in SG2 provides a ^{14}C age of 370 ± 20 yrs BP, which, when calibrated to calendar years[29], has a 2-σ uncertainty range between 1451 and 1629 CE.

Flood Deposit Chronology. Tide gauge records identify 6 floods with storm tides greater than 2 m at the Battery since archived records begin in 1844 CE[8]. In order of CE age, and with their respective storm tides, these top flood years include 1865 (2.1 m), 1950 (2.1 m), 1953 (2.2 m), 1960 (2.3 m), 1992 (2.2 m) and 2012 (3.4 m). Other documentation provides further evidence of significant floods at the Battery in 1693, 1788, 1821, and potentially 1893[7].

Below the surficial Hurricane Sandy deposit, additional anomalously dense event layers are evident down to the base of the core. In particular, the first prominent deposit below the industrial onset is a 4 cm thick deposit ending at a sediment depth of 121 cm, and with a median age for this depth that dates almost exactly to the 1821 hurricane (1823 CE, Fig. 3). Below the 1821 deposit, additional event layers at 129 and 159 cm also date to the timing of the early historical hurricanes in 1788 and 1693, respectively (median ages of 1789 CE and 1691 CE). A less prominent deposit is evident just below the industrial onset at 116 cm that dates roughly to 1865 (median age of 1852 CE), and is consistent with the timing of the largest storm tide reported within archived tide gauge data between 1844 and 1900[8]. Note that the median derived age for the deposit at 116 cm is more consistent with the 1865 flood than with the 1893 storm, which is just outside of the 2-σ uncertainty bounds of this deposit (Fig. 3). Thus an event deposit for the 1893 hurricane is noticeably absent from the record, which is consistent with archival tide gauge data that downgrades the flood magnitude of this event in New York Harbor[8].

Two of the most prominent deposits in SG2 that date to the 1900s occur at a depth of 47 and 70 cm. The deeper of these two deposits resides between the 1954 and 1963 CE onset and peak in ^{137}Cs, and is consistent with the timing of Hurricane Donna in 1960. The origin of the shallower deposit at 47 cm is less clear but is within the 1-σ age uncertainty for the December Nor'easter of 1992, which represents the largest storm tide recorded at the Battery falling between Hurricane Donna in 1960 and Sandy in 2012. Finally, two additional deposits occur just below the 1954 onset of ^{137}Cs at 83 and 85 cm with ages that are consistent with floods in 1953 and 1950. In addition to the 1865, 1960, 1992 and 2012 storms, these two 1950s floods are the

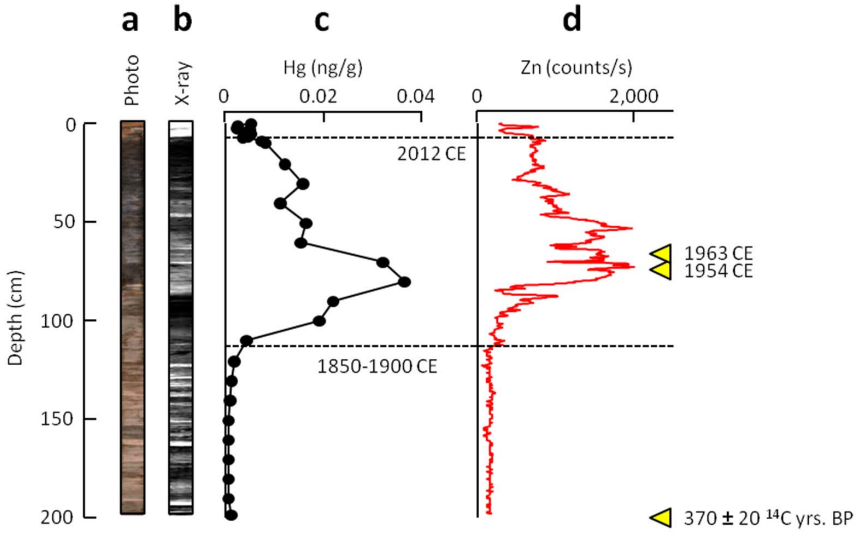

Figure 2 | Core SG2 Age Constraints. (a) Optical photograph of SG2 showing red event beds, with the Hurricane Sandy deposit at the surface. (b) X-radiograph showing density variations in the core. White areas are denser than black and generally correspond to event deposits. (c) Mercury (Hg) and (d) Zinc (Zn) abundances. The upper dashed line indicates the base of the Hurricane Sandy deposit or 2012 CE. The lower dashed line marks the initial rise in heavy metals accompanying the onset of the Industrial Revolution (1850–1900 CE). In d, the yellow triangles indicate three more dating horizons: the 1963 peak in ^{137}Cs abundance due to atmospheric nuclear weapons testing, the 1954 onset of ^{137}Cs, and a radiocarbon date indicating an age range between 1451 and 1629 CE.

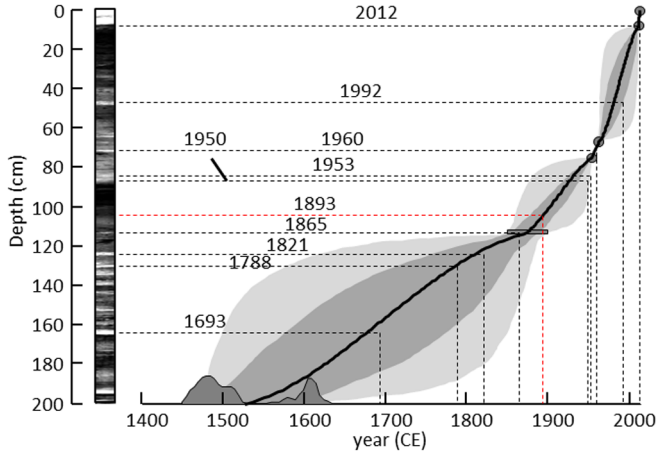

Figure 3 | Bayesian analysis using chronological constraints from core SG2. The 1-σ age range is shown in medium gray and the 2-σ age range in light gray. ^{14}C age probabilities are shown in dark gray just above the x-axis. The dark gray bar corresponds to the 1850–1900 onset of industrial heavy metals and circles indicate known ages based on ^{137}Cs and the depth of the 2012 Sandy deposit (Fig. 2). Vertical dashed lines correspond to the dates of significant surge events in New York Harbor and the horizontal dashed lines indicate their most likely deposit (seen in the x-radiograph). The 1893 event (red dashed lines) does not have a corresponding deposit.

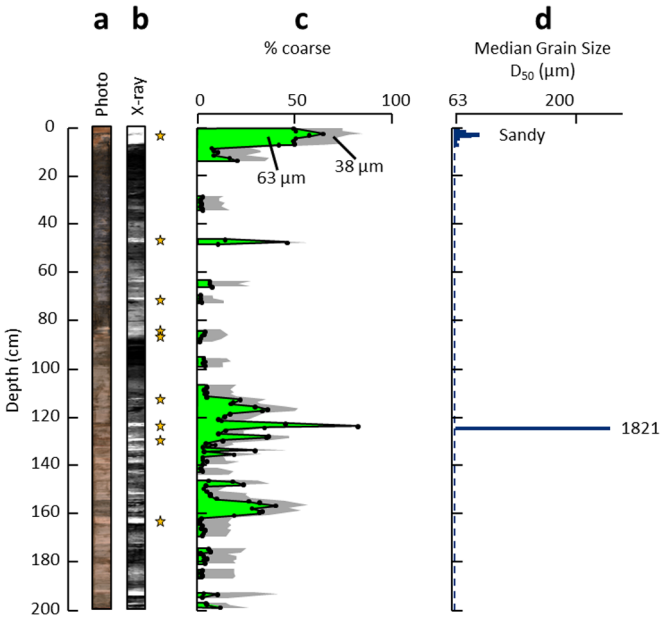

Figure 4 | Sedimentary characteristics of storm deposits in core SG2. (a) Optical photograph of SG2 showing red flood derived deposits. (b) X-radiograph showing increased density of deposits. Deposits are indicated with orange stars. (c) Percentage of coarse material in each deposit. The percentage greater than 63 μm is shown in green and the percentage greater than 38 μm is shown in gray. (d) Median grain size (D_{50}) for deposits greater than 63 μm. The dashed blue line is the 63 μm sieving limit.

only other events since 1844 when storm tides exceeded 2 m at the Battery[8]. All historical flood events in excess of a 2 m storm tide at the Battery therefore appear to be accounted for in core SG2, along with early historical hurricanes in 1693, 1788, and 1821.

Grain Size Analyses. Percent sand and grain size analyses of event deposits in Core SG2 are presented in Figure 4. The 1821 CE deposit emerges as the coarsest deposit observed in SG2 with 82% sand (i.e. grain size fraction >63 μm), followed by Hurricane Sandy with 65% sand. In terms of percent >38 μm, Hurricane Sandy and the 1821 events are roughly equivalent at 85% and 86%, respectively. Hurricane Sandy and the 1821 deposit are also the only two event layers in core SG2 with a median grain size >63 μm (Fig. 4d). All other samples are less than 50% sand, such that their D_{50} grain sizes were less than the 63 μm sieving limit.

The D_{50} grain size for the 1821 hurricane was 240 μm, over two times larger than Hurricane Sandy's D_{50} of 90 μm. It is possible that the anomalously large grain sizes of the 1821 event are due to the dilution of coarse material with fines in the Hurricane Sandy deposit. However, the D_{90} values of just the sand fraction (see Methods) show that the 1821 hurricane remains the coarsest event with a 480 μm D_{90} grain size, compared to a D_{90} of 220 μm for Hurricane Sandy's event layer. Thus, when considering just the sand size fraction, peak grain sizes within the 1821 deposit are still over twice as great as that observed within Hurricane Sandy sediments, thereby ruling out fine grained dilution as the sole reason for the smaller grain sizes observed in Hurricane Sandy's event layer.

Spatial Trends in Deposition. Deposition associated with Hurricane Sandy is evident in all four cores obtained from Seguine Pond (Fig. 5). Grain size remains relatively uniform in the vertical for the Sandy deposit at each of the sampling locations (i.e. no vertical grading), but with clear sorting trends in the horizontal (Fig. 6). The Sandy deposit is thickest in the core closest to the barrier (SG1) at 20 cm and thins monotonically landward to 8 cm, 6 cm, and 5 cm in cores SG2, SG3, and SG4, respectively. When sieved, the grain size of the deposit fines landward, with the greatest percent sand observed in SG1 at 89%, and decreasing to 65%, 39%, and 33% in SG2, SG3, and SG4, respectively (Fig. 6a). The D_{90} grain size also decreases landward, going from 470 μm in SG1 to 220 μm in SG2, and 190 μm in both SG3 and SG4.

Similar to deposition from Hurricane Sandy, the 1821 deposit also decreases in thickness landward from a maximum of 11 cm in core SG1, to 5 cm in both SG2 and SG3, and 2 cm in core SG4 (Fig. 6a). A similar general fining trend is observed in grain size within the 1821 deposit (Fig. 6b). Although D_{90} grain size initially coarsens from 410 μm at SG1 to 450 μm in SG2, this is followed by a steady fining to 420 μm and 410 μm for cores SG3 and SG4, respectively. Sieve results reveal a similar pattern with 46% sand in SG1, increasing to 82% in SG2, and then decreasing to 37% in SG3 and 9% in SG4.

Constraints on Storm Intensity. Both the Hurricane Sandy and the 1821 deposits generally fine and thin landward, while exhibiting little distinguishable vertical grading (Fig. 6). These patterns in lateral sorting are similar to those observed within other storm deposits collected from previous back-barrier ponds, and consistent with depositional trends governed predominantly by the settling of particles out of suspension while being advected landward by waves[18,30]. For such storm deposits, observed trends in grain size and thickness have in the past provided additional information for constraining flood conditions.

Ref. 15 observed a scaling between peak storm surge height and the maximum grain size within storm deposits from a coastal sinkhole in Apalachee Bay, FL. This site was far inland with surge likely the primary governor of flow. However, the D_{90} grain size of the 1821 event deposit at Seguine Pond is over twice that of Hurricane Sandy, while earlier documentation suggests a similar storm tide for the two events[5,7]. Therefore, either the 1821 event was substantially greater than that reported in the early documentation or some process other than overall storm tide is the primary governor of transport competence (i.e. the maximum grain sizes capable of being transported by a flow) during inundation at the site.

An alternative control on transport competence includes the wave climate during barrier inundation, which governs the higher fre-

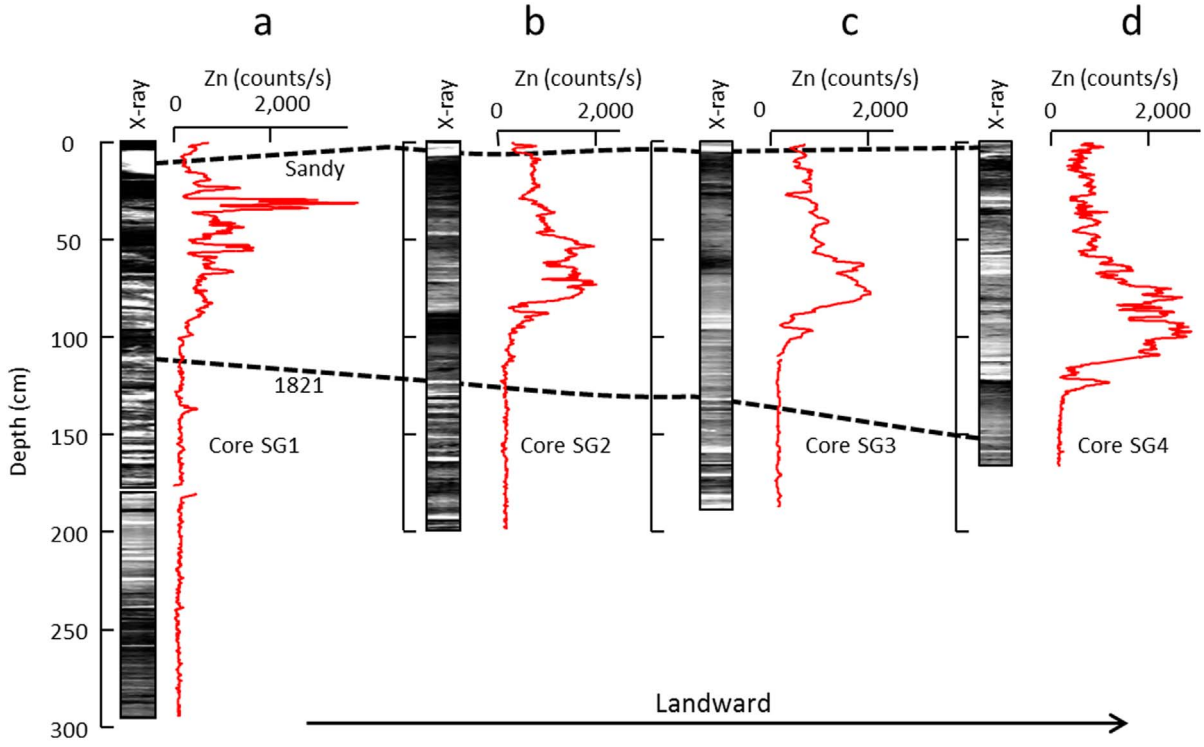

Figure 5 | Core Transect from Seguine Pond. X-radiographs and Zn abundance (red lines) of (a) Core SG1, the core closest to the barrier, (b) core SG2, (c) core SG3, and (d) core SG4. Deposits associated with Hurricane Sandy and the 1821 hurricane deposits are indicated with the dashed lines.

quency oscillations in the flow that likely produce peak shear stresses[31]. Ref. 30, observed a scaling between the magnitude of excess wave run-up over a barrier and the maximum grain size observed in landward fining, back-barrier deposits along the coast of Vieques, Puerto Rico (where run-up is defined as the maximum wave-induced uprush of water on a beach above still water). Here the greatest transport competence is assumed to occur when waves breach and inundate the barrier via low-frequency infra-gravity waves[32], which then flood the pond as bores[31]. Under such flooding conditions ref. 30 relates maximum wave-induced run-up over the barrier (R_{max}) to maximum grain size at a sampling site with:

$$R_{max} = \left(\frac{x_L^2 w_S^2}{g}\right)^{1/3} + h_b \quad (1)$$

where g is the acceleration due to gravity, h_b is the barrier height, and w_s is the settling velocity of the peak grain size advected landward a distance of x_L from the barrier. Here we define the maximum grain size with D_{90} and convert to settling velocity using the grain size vs. particle settling velocity relationship presented in ref. 33. Using the observed D_{90} of 220 μm for the Hurricane Sandy deposit at SG2 and an average barrier height of 1.5 m for the site, equation (1) results in a R_{max} of 2.1 m. Significant offshore wave heights (H_o) during Hurricane Sandy near landfall are documented at 9.9 m with a dominant wave period of 13.8 s[34], and respective offshore wavelength (L_o; ref. 32) of roughly 300 m. Resulting off-shore wave steepness likely results in dissipative breaking conditions[32], where wave run-up has been empirically related to H_o and L_o as:

$$R_{max} = \alpha (H_0 L_0)^{1/2} \quad (2)$$

with a best fit α of 0.043. This relationship provides a predicted wave run-up of 2.3 m for Hurricane Sandy, which is quite close to the run-up of 2.1 m independently derived based on the D90 grain size of the Hurricane Sandy deposit at SG2.

The advective-settling model proposed by ref. 30 is certainly an over-simplification of the overwash process; however, similar independent run-up predictions between it and that predicted by equation (2) for Hurricane Sandy provide support for the model's use in obtaining a rough estimate of run-up and respective storm conditions for the 1821 hurricane. Using equation (1), a D_{90} of 450 μm at SG2 for the 1821 deposit results in a predicted R_{max} of 2.6 m. Wave periods and resultant off-shore wave lengths for the 1821 event are unavailable but assumed similar to Hurricane Sandy with a L_o of 300 m. In turn, equation (2) provides an off-shore significant wave height of roughly 12 m for an R_{max} of 2.6 m. Ref. 35 proposes the following empirical relationship between severe wind speed (U_{wind}) and significant off-shore wave height:

$$H_0 = 0.235\ U_{wind} \quad (3)$$

Using an estimated H_o of 12 m for the 1821 hurricane, equation (3) provides a respective wind speed of 51 m/s, roughly equivalent to a weak category 3 hurricane[36]. This intensity is also consistent with earlier assessments for the strength of the 1821 hurricane based on independent documentation of wind damage occurring during the event[5,6].

SLOSH simulations of the 1821 hurricane. Accounts of the 1821 event describe a storm surge of ~4 m inundating the Battery in just 1 hour[4]. However, it is unclear if a storm estimated as a weak, category 3 intensity would be capable of such a rapid rise in water. To further test this we perform storm surge simulations of the event using NOAA's Sea, Lake, and Overland Surges from Hurricanes (SLOSH) model[37] (see Methods section for details).

The documentary evidence suggests the 1821 hurricane was considerably smaller in size than Hurricane Sandy. Ref. 4 describes the size of the storm, based on reports of wind damage, as "...confined

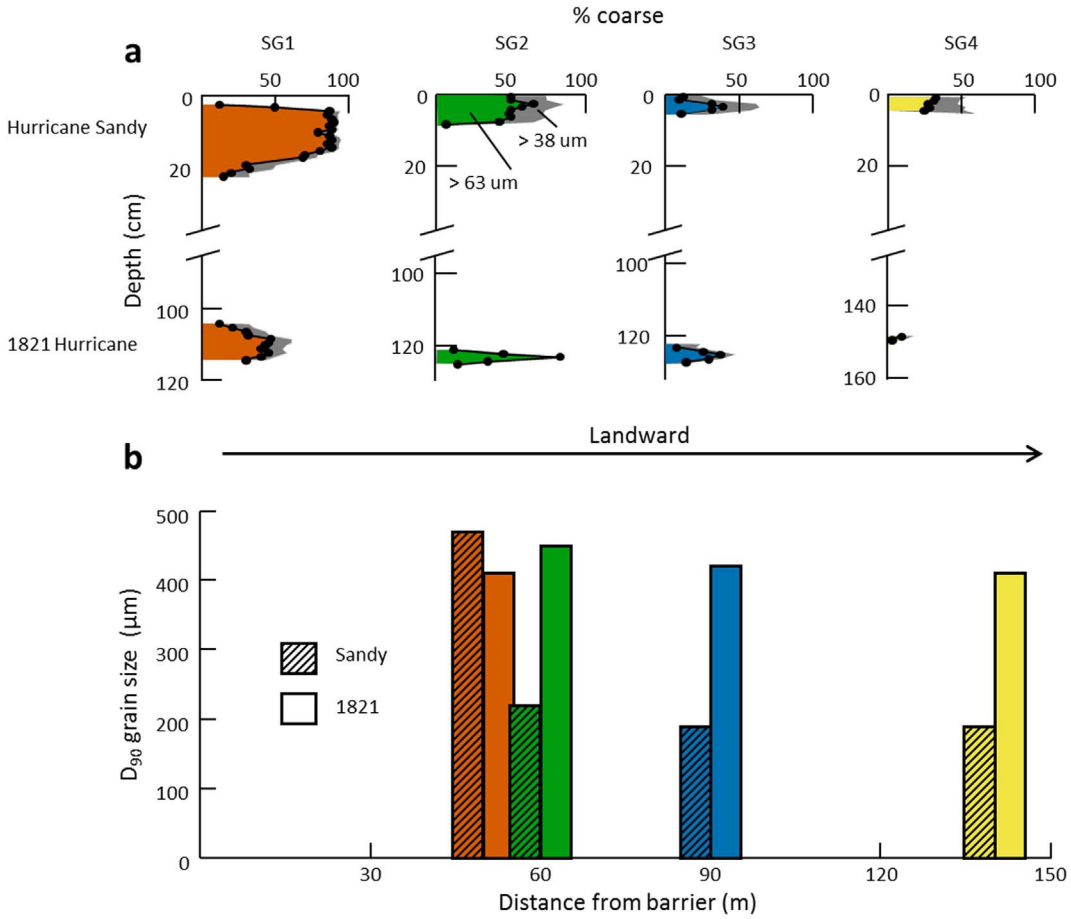

Figure 6 | Hurricane Sandy vs. 1821 Hurricane Deposition. (a) Percent coarse of the Hurricane Sandy and 1821 hurricane deposits in each core taken from Seguine Pond. The percentage of material >63 μm is in color and the percentage >38 μm is in gray. Core order starts closest to the barrier and extends landward (left to right). (b) D_{90} grain size of the Hurricane Sandy (striped) and 1821 (solid) deposits in each core. Colors correspond to the same cores as in (a) and are shown in relative distance from the barrier.

within a circuit whose diameter does not appear to have greatly exceeded one hundred miles," or, therefore, having an 80 km radius. Ref. 38 computes the radius of maximum winds as 31 miles (50 km) and report observations ranging from 30–40 miles (48–64 km) for this storm. The discrepancy between these two records is most likely due to their description of two different aspects of the storm with ref. 4 describing the diameter of the damaging winds and ref. 38 describing the radius of maximum wind speed. For comparison, a radius of maximum wind of just 50 km for the 1821 event is 3–4 times smaller than the size of Hurricane Sandy, which had a radius of maximum wind of 160–200 km near landfall.

The track and translation speed of the 1821 hurricane is fairly well constrained due to the large number of historical accounts of its passage[4–6]. Based on these observations, the 1821 storm was likely moving substantially faster than Hurricane Sandy with an estimated translation speed of 61 km/hr[38] (or 64 km/hr using ref. 39), compared to 29 km/hr for Sandy.

Because the above parameters are not precisely known, storm surge simulations for the 1821 event were run using a range of storm sizes, central pressure differences, and translation speeds. The simulation of the 1821 hurricane that most closely reproduced the rapid rise in water level had a radius of maximum winds of 40 km, 58 m/s (~210 km/hr) sustained winds, and a translation speed of 65 km/hr, which is generally consistent with historical observations described above (Fig. 7). Storm surge simulation of these hurricane conditions results in a rise in water of roughly 4 m but over an interval of two hours rather than one. However, these simulations provide support for the magnitude of storm surge of roughly 4 m noted in the documentary record for the 1821 event, which is substantially greater than the 2.8 m of surge observed during Hurricane Sandy.

Discussion

Sedimentological dissimilarities between the 1821 and Hurricane Sandy deposits highlight the different nature of the two flooding events. While the 1821 deposit is the coarsest event layer observed in Seguine Pond, the resultant deposition by Hurricane Sandy is consistently the thickest deposit at the site (Fig. 6), with thickness potentially related to the total net transport into the pond during an event[40]. The volume of sediment that overwashes a barrier during a flood event is related to the time-varying rate of overwash transport and the duration of flooding[41]. Overwash sediment transport rates are commonly assumed to be a function of excess wave run-up[31,41], while flood duration is more related to the size and speed of the storm[42–44]. Larger and slower storms like Hurricane Sandy (translation speed of 29 km/hr and a radius of maximum winds of 160–200 km), therefore have significantly longer flood durations than that documented for the smaller and faster moving 1821 event (translation speed of 65 km/hr and radius of maximum winds of 40 km). In turn, the anomalous thickness of the Hurricane Sandy deposit relative to past flood layers preserved at the site is consistent with greater net transport during the 2012 event. Thus although significantly larger grain sizes for the 1821 deposit point to greater initial wave run-up and overall storm intensity, Hurricane Sandy's anomalous thickness relative to the 1821 deposit supports Hurricane Sandy being significantly greater in size and of significantly longer flood duration (Fig. 7).

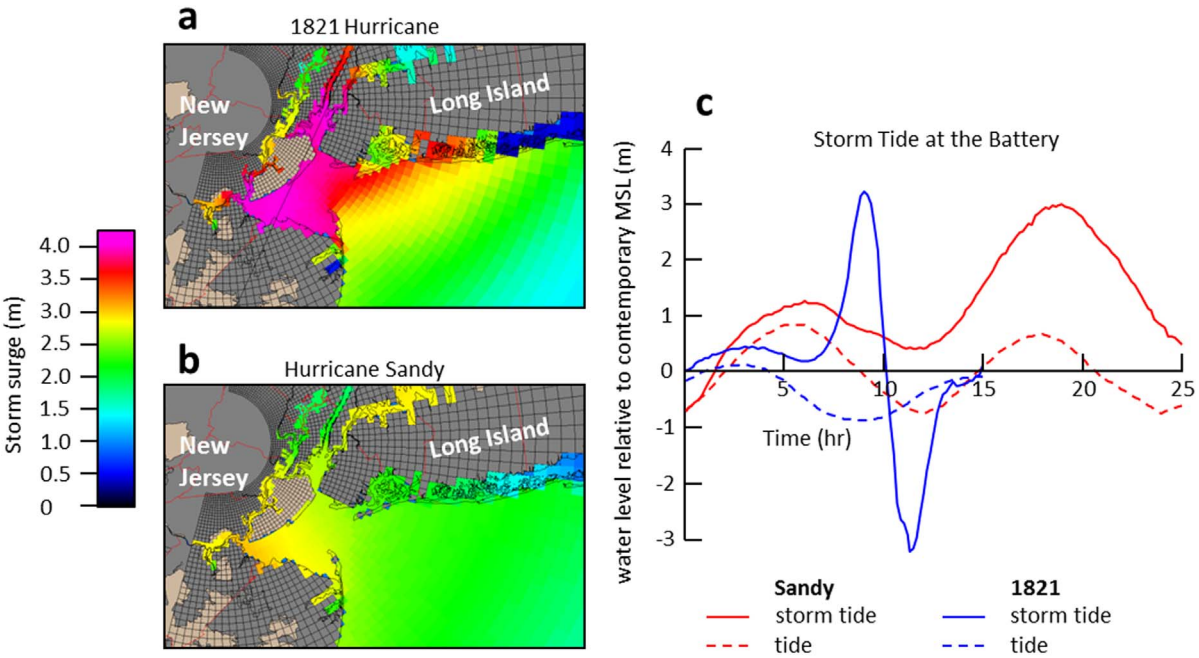

Figure 7 | SLOSH model results of storm surge (i.e. not adjusted for tides) for (a) the 1821 hurricane and (b) Hurricane Sandy. Maps were generated using the SLOSH Display program (1.66a). (c) Tides (dashed lines) and storm tides (solid lines) for the 1821 hurricane (blue) and Hurricane Sandy (red). The beginning of the inundation for both storms is set to 0.

The return period of Hurricane Sandy's 3.4 m storm tide at the Battery has been estimated to range between 900[2] and 1600[1] years. The probability that this event could occur during the last century can be calculated using

$$P = \frac{n!}{x!(n-x)!} p^x q^{n-x} \quad (4)$$

where n is the interval of time under consideration, x is the number of occurrences of the event, p is the probability of "success" (i.e. the event happens) and q is the probability of "failure" (i.e. the event doesn't happen)[45]. Using the length of the instrumental period and a 1000 year storm (i.e. p = 1/1000 or 0.001), the probability of an event like Hurricane Sandy occurring during the last century is roughly 10%[46]. However, the probability of two 1000-year storm tides occurring over three successive centuries (i.e. similar storm tides for Hurricane Sandy and the 1821 hurricane over the length of the sediment record), is ~3%. The assessment serves to highlight the difficulties and large uncertainty associated with accurately assessing the return period for an event of Hurricane Sandy's magnitude, and the value of extending records beyond the instrumental with natural archives such as those provided by the Seguine Pond reconstruction.

Relative sea-level change is an environmental factor that could affect sedimentation at the field site. However, the percent coarse fraction of deposits in core SG2 does not exhibit any systematic increases or decreases up core (Fig. 4c). A similar trend was observed within previous overwash reconstructions[30], and provides support for a relatively stable barrier system in recent centuries in the face of relatively modest rates of sea-level rise[46,47]. Assuming that barrier elevation has risen at a rate similar to regional rates of sea-level, variations between flood deposits in Seguine Pond likely represent differences in storm characteristics relative to sea-level at the time of flooding.

Documented accounts of flooding for the 1821 hurricane are also likely in reference to mean low water at the time of flooding[5] with the resulting storm tide of 3.2–3.4 m relative to 1821 MSL. An analysis of long-term trends with tide gauge data at the Battery reveals an average rate of sea-level rise of 2.77 mm/yr since records begin in 1856 CE[48]. Extrapolating this rate back to 1821 suggests roughly 0.5 m of sea-level rise between the 1821 hurricane and Hurricane Sandy in 2012. Independent evaluations of sea-level rise from marsh records result in a similar rate of 2.5 mm/yr or ~0.48 m since 1821[47]. Relative to the datum of modern mean sea level, the 1821 hurricane's peak water levels would have been 0.5 m lower or 1.7–1.9 m above modern mean sea level. Further, in terms of total storm surge the 1821 flood probably exceeded that of Hurricane Sandy significantly: 4.0 m for the 1821 Hurricane relative to 2.8 m for Hurricane Sandy. Therefore, when compared to the 1821 Hurricane, Sandy's record breaking water level likely has more to do with its occurrence at high tide and the increase in mean sea-level since 1821.

In summary, an inundation record covering the past ~300 years was reconstructed from sediment cores taken from New York City, NY. Deposits in the record correspond to storms known to have affected New York Harbor, including early historic storms in 1693, 1788, and 1821. Sedimentary analysis reveals only two deposits, those of Hurricane Sandy and the 1821 hurricane, with a median grain size in the sand range (>63 μm). While the Hurricane Sandy deposit was much thicker than the 1821 deposit, it had a smaller maximum grain size. This is consistent with historic accounts and SLOSH model results that suggest that the 1821 hurricane was a smaller (radius of maximum winds of 40 km) but significantly more intense storm (maximum 1-minute sustained wind speed of ~210 km/hr), compared to Hurricane Sandy with a radius of maximum winds of 160–200 km and 130 km/hr sustained winds at landfall. Sea-level rise and peak surge occurring at high tide combined to give Sandy record-breaking water levels, but the 1821 hurricane probably had a significantly larger overall storm surge. Our results indicate that extreme flood events like Hurricane Sandy are not uncommon within sedimentary records and that the true return interval for such extreme events to New York City is probably significantly shorter than current estimates.

Methods

Field work. All cores were collected using a modified Vohnout/Colinvaux piston core following methods similar to ref 26. Beginning closest to the barrier and traversing landward, cores and locations include SG1 (N 40.52423°, W 74.16934° ± 4 m), SG2

(N 40.52438°, W 74.16921° ± 3 m), SG3 (N 40.52463°, W 74.16919° ± 4 m), and SG4 (N 40.52506°, W 74.16908° ± 4 m).

Analysis of sediment cores. X-radiograph images were initially obtained on all cores by scanning split sections at 500 μm resolution on an Itrax Core Scanner[49]. Black and white inverted x-radiographs reveal density variations in all cores and anomalously dense bands are used as a proxy for event-driven deposition by storms[13–15]. Core SG2 was chosen for detailed sedimentary analysis due to its central location in the pond[12] and the abundance of well-preserved storm layers. Following identification with the x-radiographs, the dense layers in core SG2 were subsampled at 1 cm intervals. Samples were weighed, dried in an oven at 100 °C for 24 hours, and weighed again to determine the mass of water. Dried samples were then powdered using a mortar and pestle and transferred to ceramic crucibles. The crucibles were put in a muffle furnace for 2 hours at 550 °C to combust organic material.

Following combustion, samples were transferred to plastic vials, hydrated, and sonicated for 3 hours to disaggregate clay particles. Next, they were wet sieved at both 63 μm, corresponding to the transition between sand and silt[50], and 38 μm, which is near the coarse silt to medium silt transition. Retained samples were then dried at 100 °C for 24 hours to obtain the mass of the sand fraction (>63 μm) and the mass of the approximate coarse silt fraction (<63 μm and >38 μm).

The coarse (>63 μm) fraction was run through a digital image processing, size and shape analyzer (Retsch Technology Camsizer) with the size distribution analyzed for both percent coarse (unadjusted) and adjusted for the removed fines[15]. Grain size results presented in this study include the median (D_{50}) grain size and the size of the largest subset of grains in the sample, taken as D_{90}, or the size for which 90% of the particles in the size distribution are finer. Two grain size distributions are considered: the total distribution of all grain sizes in a sample and the grain size distribution of just the sand fraction. In this study, we present the D_{50} grain size of the total grain size distribution, but the D_{90} grain size of just the sand fraction. The D_{90} grain size is similar between the unadjusted and adjusted distributions but we believe that using the unadjusted D_{90} grain size in the transport competence calculations is more representative of largest grain sizes transported to the location during flooding.

Dating techniques. Temporal constraints on sediment deposition were determined using radiocarbon, cesium-137 (^{137}Cs), and the onset of industrial heavy metals (as identified in concentration-depth profiles of Hg and Zn). The global onset of ^{137}Cs in the sediment record corresponds to 1954 CE, or the start of atmospheric nuclear weapons testing, and the peak in ^{137}Cs dates to 1963 CE, or just prior to the signing of the Nuclear Test Ban Treaty[25]. ^{137}Cs was measured using a Canberra GL2020R Low Energy Germanium Detector. Sediment samples with a dry mass greater than 2 grams were powdered, put in 6 cm diameter plastic jars, and counted for 48–96 hours. ^{137}Cs activities were computed spectroscopically using the 661.7 keV photopeak.

In the Northeastern U.S., concentrations of heavy metals increase significantly in sediment between 1850 and 1900 CE, corresponding to the rise of factories during the Industrial Revolution[26–28]. Depth profiles of Hg and Zn were employed to identify the depth of this industrial horizon. Hg measurements were obtained on dried sediments from core SG2 with a Teledyne Leeman Labs Hydra-C mercury analyzer following procedures described by ref. 26. Zn activities were measured in all cores with the ITRAX Core Scanner using a Molybdenum tube and operating at 30 kV and 55 mA for 10 seconds per measurement, and at a 500 μm resolution. To extend ages beyond heavy metal and ^{137}Cs derived constraints, a radiocarbon date was obtained at a sediment depth of 200 cm from the SG2 core site. The radiocarbon age with 1 sigma uncertainties was converted to calendar age probabilities using the IntCal13 radiocarbon calibration curve[29].

We employ Monte Carlo simulations similar to refs. 51 and 52 to derive Bayesian age constraints between chronological controls in core SG2. For each of the large number of simulations a discrete age is drawn randomly from the sample's obtained probability radiocarbon-derived distribution. A specific age is defined for the 1963 CE and 1954 CE ^{137}Cs constraints, and a randomly drawn age between 1850 and 1900 CE for the heavy metal onset, with probabilities evenly distributed over this 1850–1900 CE interval. A date of 2012 CE was also defined at the base of the surficial deposit associated with Hurricane Sandy. Random ages were generated at random depths between the radiocarbon, ^{137}Cs, heavy metal, and Hurricane Sandy control points such that ages increase monotonically with depth (i.e. no age reversals). The median of all simulations for a particular depth is defined as the most likely age, with bounds presented for 68% and 95% uncertainties.

SLOSH model. The SLOSH model is a coastal inundation model used by the National Weather Service for storm surge inundation prediction and hindcasting[37]. The user can "create" a hurricane in the model by inputting a track, translation speed, central pressure difference (between the hurricane's eye and the ambient atmosphere), and radius of maximum winds. The central pressure difference and radius of maximum winds yield a pressure gradient body force and a resultant time-varying, surface wind field. This, along with the translation speed and track, acts as the driving force to the ocean's surface. Finally, the storm surge is modeled by solving differential equations governing fluid motion using finite-difference methods[37].

Hurricane Sandy's parameters are readily available[53] and when input into SLOSH yield a storm surge at the Battery that is ~20 cm lower than the reported surge (<10% error). While the track and translation speed are well constrained for the 1821 hurricane[4–6], the radius of maximum winds and central pressure difference are less so. To refine constrains on these parameters, numerous SLOSH model runs were executed with different combinations of these two parameters within bounds set by historical observations of the storm. The combination that best reproduces the 1821 storm tide height and inundation period as documented by ref. 4 at the Battery is presented in Fig. 7.

1. Sweet, W., Zervas, C., Gill, S. & Park, J. Hurricane Sandy inundation probabilities today and tomorrow. *Bull. Am. Meteorol. Soc.* **94**, S17–S20 (2013).
2. Lin, N., Emanuel, K. A., Oppenheimer, M. & Vanmarcke, E. Physically based assessment of hurricane surge threat under climate change. *Nature Clim. Change* **2**, 462–467 (2012).
3. Irish, J. L., Youn, K. S. & Chang, K.-A. Probabilistic hurricane surge forecasting using parameterized surge response functions. *Geophys. Res. Lett.* **38**, L03606 (2011).
4. Redfield, W. C. Remarks on the prevailing storms of the Atlantic Coast of the North American States. *Am. J. Sci.* **20**, 17–51 (1831).
5. Ludlum, D. M. *Early American Hurricanes.* (American Meteorological Society, Boston, 1963).
6. Boose, E. R., Chamberlin, K. E. & Foster, D. R. Landscape and regional impacts of historical hurricanes in New England. *Ecol. Monogr.* **71**, 27–48 (2001).
7. Scileppi, E. & Donnelly, J. P. Sedimentary evidence of hurricane strikes in western Long Island, New York. *Geochem. Geophys. Geosyst.* **8**, Q06011 (2007).
8. Talke, S. A., Orton, P. & Jay, D. A. Increasing storm tides in New York Harbor, 1844–2013. *Geophys. Res. Lett.* **41**, 3149–3155 (2014).
9. Zervas, C. *Extreme water levels of the United States 1893–2010 NOAA Technical Report NOS CO-OPS 067.* <http://tidesandcurrents.noaa.gov/publications/NOAA_Technical_Report_NOS_COOPS_067a.pdf>, (2013) Date of access: 18/10/2014.
10. Donnelly, J. P. *et al.* 700 yr sedimentary record of intense hurricane landfalls in southern New England. *Geol. Soc. Am. Bull.* **113**, 714–727 (2001).
11. Donnelly, J. P. *et al.* Sedimentary evidence of intense hurricane strikes from New Jersey. *Geology* **29**, 615–618 (2001).
12. Donnelly, J. P. & Woodruff, J. D. Intense hurricane activity over the past 5,000 years controlled by El Niño and the West African monsoon. *Nature* **447**, 465–468 (2007).
13. Boldt, K. V., Lane, P., Woodruff, J. D. & Donnelly, J. P. Calibrating a sedimentary record of overwash from Southeastern New England using modeled historic hurricane surges. *Mar. Geol.* **275**, 127–139 (2010).
14. Lane, P., Donnelly, J. P., Woodruff, J. D. & Hawkes, A. D. A decadally-resolved paleohurricane record archived in the late Holocene sediments of a Florida sinkhole. *Mar. Geol.* **287**, 14–30 (2011).
15. Brandon, C. M., Woodruff, J. D., Lane, D. P. & Donnelly, J. P. Tropical cyclone wind speed constraints from resultant storm surge deposition: A 2500 year reconstruction of hurricane activity from St. Marks, FL. *Geochem. Geophys. Geosyst.* **14**, 2993–3008 (2013).
16. Denommee, K. C., Bentley, S. J. & Droxler, A. W. *Climatic controls on hurricane patterns: a 1200-y near-annual record from Lighthouse Reef, Belize.* Sci. Rep. **4**, 3876; Doi: 10.1038/srep03876 (2014).
17. Wallace, D. J. & Anderson, J. B. Evidence of similar probability of intense hurricane strikes for the Gulf of Mexico over the late Holocene. *Geology* **38**, 511–514 (2010).
18. Donnelly, J. P., Butler, J., Roll, S., Wengren, M. & Webb, T. A backbarrier overwash record of intense storms from Brigantine, New Jersey. *Mar. Geol.* **210**, 107–121 (2004).
19. Borns, H. W. Jr. Late Wisconsin fluctuations of the Laurentide ice sheet in southern and eastern New England. In *The Wisconsin Stage* [Black, R. F., Goldthwait, R. P. & Williman, H. B. (eds.)], (37–45), (GSA Memoirs **136**, Boulder, CO, 1973).
20. Soren, J. *Geologic and geohydrologic reconnaissance of Staten Island, New York U.S. Geologic Survey, Water-Resources Investigations Report* 87–4048. <http://pubs.usgs.gov/wri/1987/4048/report.pdf>, (1988) Date of access: 06/01/2014.
21. Garin, J. *et al.* Bluebelt beginnings – green preserves blue on Staten Island. *Clear Waters* **39**, 10–20 (2009).
22. Blake, E. S., Kimberlain, T. B., Berg, R. J., Cangialosi, J. P. & Beven, J. L. II. *Tropical Cyclone Report: Hurricane Sandy.* National Hurricane Center **12**, <http://www.nhc.noaa.gov/data/tcr/AL182012_Sandy.pdf > (2013) (Date of access: 01/05/2014).
23. United States Geological Survey, *Coastal Change Hazards: Hurricanes And Extreme Storms.* <http://coastal.er.usgs.gov/hurricanes/sandy/field-measurements/>, (2014) (Date of access: 05/06/2014).
24. Yellen, B. *et al.* Source, conveyance and fate of suspended sediments following Hurricane Irene. New England, USA. *Geomorphology* **226**, 124–134 (2014).
25. Pennington, W., Tutin, T., Cambray, R. & Fisher, E. Observations on lake sediments using fallout 137Cs as a tracer. *Nature* **242**, 324–326 (1973).
26. Woodruff, J. D. *et al.* Off-river waterbodies on tidal rivers: human impact on rates of infilling and the accumulation of pollutants. *Geomorphology* **184**, 38–50 (2013).
27. Varekamp, J. C., Mecray, E. L. & Maccalous, T. Z. Once spilled, still found: metal contamination in Connecticut coastal wetlands and Long Island Sound sediment from historic industries. In *America's Changing Coasts: Private Rights And Public Trust.* [Whitelaw, D. M. & Visgilio, G. R. (eds.)] (Edward Elgar Publishing, Inc., Northampton, MA, 2005).

28. Varekamp, J., Kreulen, B., Buchholtz ten Brink, M. R. & Mecray, E. Mercury contamination chronologies from Connecticut wetlands and Long Island Sound sediments. *Environ. Geol.* **43**, 268–282 (2003).
29. Reimer, P. J. *et al.* IntCal13 and Marine13 radiocarbon age calibration curves 0–50,000 years cal BP. *Radiocarbon* **55**, 1869–1887 (2013).
30. Woodruff, J. D., Donnelly, J. P., Mohrig, D. & Geyer, W. R. Reconstructing relative flooding intensities responsible for hurricane-induced deposits from Laguna Playa Grande, Vieques, Puerto Rico. *Geology* **36**, 391–394 (2008).
31. Donnelly, C. K., Kraus, N. & Larson, N. M. State of knowledge of measurement and modeling of coastal overwash. *J. Coastal Res.* **22**, 965–991 (2006).
32. Stockdon, H. F., Holman, R. A., Howd, P. A. & Sallenger, A. H. Jr. Empirical parameterization of setup, swash, and runup. *Coast. Eng.* **53**, 573–588 (2006).
33. Ferguson, R. I. & Church, M. A simple universal equation for grain settling velocity. *J. Sediment. Res.* **74**, 933–937 (2004).
34. National Data Buoy Center, *Station 44065 (LLNR 725) — New York Harbor Entrance — 15 NM SE of Breezy Point, NY*. <http://www.ndbc.noaa.gov/station_page.php?station=44065>, (2014) (Date of access: 06/06/2014).
35. Ochi, M. K. *Ocean Waves: The Stochastic Approach.* (Cambridge University Press 6, New York, 2005).
36. Saffir, H. & Simpson, R. The hurricane disaster potential scale. *Weatherwise* **27**, 169–186 (1974).
37. Jelesnianski, C. P., Chen, J. & Shaffer, W. A. *SLOSH: Sea, Lake, and Overland Surges from Hurricanes.* <http://slosh.nws.noaa.gov/sloshPub/pubs/SLOSH_TR48.pdf>, (1992) Date of access: 15/04/2014.
38. Graham, H. E. & Hudson, G. N. National Hurricane Research Project Report No.39: Surface winds near the center of hurricanes (and other cyclones). *U. S. Department of Commerce* (1960).
39. Landsea, C. W. *et al.* The Atlantic hurricane database re-analysis project: documentation for the 1851–1910 alterations and additions to the HURDAT database. In *Hurricanes and Typhoons: Past, Present, and Future.* [Murnane, R. & Liu, K. (eds.)], (177–221), (Columbia Press, New York, 2004).
40. Morton, R. A., Gelfenbaum, G. & Jaffe, B. E. Physical criteria for distinguishing sandy tsunami and storm deposits using modern examples. *Sediment. Geol.* **200**, 184–207 (2007).
41. Donnelly, C., Hanson, H. & Larson, M. A numerical model of coastal overwash. *P. I. Civil Eng.-Mar. Eng.* **162**, 105–114 (2009).
42. Davis, R. E. & Dolan, R. Nor'easters. *Am. Sci.* **81**, 428–439 (1993).
43. Weisberg, R. H. & Zheng, L. Hurricane storm surge simulations for Tampa Bay. *Estuar. Coast.* **29**, 899–913 (2006).
44. Irish, J. L., Resio, D. T. & Ratcliff, J. J. Influence of storm size on hurricane surge. *J. Phys. Oceanography* **38**, 2003–2013 (2008).
45. Gray, H. L. & Odell, P. L. *Probability for Practicing Engineers.* (Barnes & Noble, New York, 1973).
46. Woodruff, J. D., Irish, J. & Camargo, S. Coastal flooding by tropical cyclones and sea-level rise. *Nature* **504**, 44–52 (2013).
47. Kemp, A. C. & Horton, B. P. Contribution of relative sea-level rise to historical hurricane flooding in New York City. *J. Quaternary Sci.* **28**, 537–541 (2013).
48. National Oceanic and Atmospheric Administration, *Tides & Currents*. <http://tidesandcurrents.noaa.gov/waterlevels.html?id=8518750&units=standard&bdate=20121028&edate=20121030&timezone=GMT&datum=MLLW&interval=6&action=>, (2013) (Date of access: 13/01/2014).
49. Croudace, I. W., Rindby, A. & Rothwell, R. G. ITRAX: Description and evaluation of a new multi-function X-ray core scanner. In: *New Techniques in Sediment Core Analysis* [Rothwell, R. G. (ed.)], (51–63), (Geol. Soc. Lond. Spec. Publ. **267**, London, 2006).
50. Wentworth, C. K. A scale of grade and class terms for clastic sediments. *J. Geol.* **30**, 377–392 (1922).
51. Haslett, J. & Parnell, A. A simple monotone process with application to radiocarbon-dated depth chronologies. *J. Roy. Stat. Soc. C-App.* **57**, 399–418 (2008).
52. Parnell, A. C., Haslett, J., Allen, J. R. M., Buck, C. E. & Huntley, B. A flexible approach to assessing synchroneity of past events using Bayesian reconstructions of sedimentation history. *Quaternary Sci. Rev.* **27**, 1872–1885 (2008).
53. Unisys, *2012 Hurricane/Tropical Data for Atlantic.*. <http://weather.unisys.com/hurricane/atlantic/2012H/SANDY/track.dat>, (2014) (Date of access: 02/10/2014).

Acknowledgments

Funding for this work was provided by the Hudson River Foundation Expedited Grant #004/12E, the Hudson River Foundation Graduate Fellowship 02–13, the National Science Foundation (RAPID grant #1313859 and instrument and facility support via grant IF-0949313), and the Dalio Explore Fund. We thank H. Baranes, O. Beaulieu, B. Douglas, H. Kinney, M. Koerth, L. Kumpf, and C. Maio for their laboratory and field assistance and A. Martini for help with Hg analyses.

Author contributions

All co-authors were involved with planning the field expedition. C.M.B., J.D.W. and R.M.S. collected the sediment cores from the field site. C.M.B. performed the laboratory analyses, R.M.S. conducted the SLOSH model simulations of Hurricane Sandy, J.P.D. performed the SLOSH runs of the 1821 hurricane, and J.D.W. developed Matlab code for the Bayesian depth-to-age model. The manuscript was co-written by C.M.B. and J.D.W. and was edited by all co-authors.

Additional information

Competing financial interests: The authors declare no competing financial interests.

How to cite this article: Brandon, C.M., Woodruff, J.D., Donnelly, J.P. & Sullivan, R.M. How Unique was Hurricane Sandy? Sedimentary Reconstructions of Extreme Flooding from New York Harbor. *Sci. Rep.* **4**, 7366; DOI:10.1038/srep07366 (2014).

This work is licensed under a Creative Commons Attribution-NonCommercial-NoDerivs 4.0 International License. The images or other third party material in this article are included in the article's Creative Commons license, unless indicated otherwise in the credit line; if the material is not included under the Creative Commons license, users will need to obtain permission from the license holder in order to reproduce the material. To view a copy of this license, visit http://creativecommons.org/licenses/by-nc-nd/4.0/